J Therm Anal Calorim (2018) 131:3105–3120
https://doi.org/10.1007/s10973-017-6708-3

Thermal kinetic analysis, theoretical thermodynamic calculations and antimicrobial activity of three new energetic materials

Ş. Betül Sopacı[1] · Hasan Nazır[2] · Erdal Emir[2] · Orhan Atakol[2] · Sevi Öz[1]

Received: 28 February 2017 / Accepted: 12 September 2017 / Published online: 27 September 2017

Abstract Three new energetic agents were synthesized using 3,5-dinitro-4-chlorobenzonitrile, sodium azide and hydrazine, which were 2,6-dinitro-4-cyano-azidobenzene (**I**), N-2,6-dinitro-cyanophenyl-hydrazine (**II**) and bis-N,N′(2,6-dinitro-4-cyanophenyl)hydrazine (**III**). These energetic substances were first characterized by elemental analysis, IR, mass, ^{1}H NMR and ^{13}C NMR spectroscopic methods. The energetic substances were studied by thermogravimetry, and it was understood that the mechanism of the thermal decomposition reactions consists of two successive exothermic thermal reactions. In the first thermal reaction, the energetic material was converted to furoxane compounds, and then, these furoxane compounds were decomposed by the second thermal reaction. Activation energies and Arrhenius pre-exponential factors of thermal responses were determined by using isothermal (Coats–Redfern) and nonisothermal/isoconvertional (Kissinger–Akahira–Sunose, Ozawa–Flynn–Wall) methods with thermogravimetry and differential scanning calorimetry (DSC) data. With these calculated values, other thermodynamic parameters reaction enthalpy, entropy changes and free energy were calculated. Formation enthalpies of the elements of the energetic substances were theoretically calculated using the CBS-4M algorithm in the Gaussian 09 program for the synthesized energetic substances. In the thermal decomposition reactions, the products were estimated with the aid of literature data and the enthalpies of explosion reactions were theoretically calculated according to the Hess Law. Besides, the exothermic energies in the first and second thermal reactions of the energetic substances were measured by DSC. The results measured by DSC were compared with the calculated theoretical results and were found to be very close to each other. In the study, antimicrobial activity was estimated to be high because energetic molecules are strained molecules, and it is possible this tension can affect the medium. According to this thought, antimicrobial activity was determined by using five different bacteria and a fungus. Antimicrobial activity values were determined by "agar dilution" method, and results were found as minimum inhibition concentration. Among the three energetic substances, 2,6-dinitro-4-cyano-azidobenzene was found to have the most active compound.

Keywords Formation enthalpy · Thermal kinetic analysis · KAS · OFW · Energetic material · Antimicrobial activity · CBS-4M

Introduction

2,4,6-trinitrochlorobenzene (picrylchloride) gives easy nucleophilic substitution reactions due to three nitro groups, because these groups are strong electron-withdrawing groups and decrease the electron density of the aromatic ring [1–6]. As it is known, the cyano group is a strong electron-withdrawing group like nitro group. Thus, 3,5-dinitro-4-chlorobenzonitrile or 2,6-dinitro-4-cyano-chlorobenzene can similarly give nucleophilic substitution reactions. In the direction of this thought, 2,6-dinitro-4-cyano-chlorobenzene was reacted in amphiprotic solvents with sodium azide and hydrazine to prepare three new

✉ Sevi Öz
sevioz@hotmail.com

[1] Department of Chemistry, Faculty of Science and Arts, Ahi Evran University, 40100 Kırşehir, Turkey

[2] Department of Chemistry, Faculty of Science, Ankara University, 06100 Ankara, Turkey

nitrogen-rich energetic agents, as shown in Scheme 1a and b.

These prepared substances are in the class of energetic substances because of the nitro and cyano groups they carry, as can be seen from the molecules. They are also rich in nitrogen, so they should be considered as a new generation energetic substance. Recently, the work on energetic materials is nourishing on the nitrogen-rich and environmentally friendly energetic substances [7–9].

There has been much work in the literature on the thermal degradation of 2,4,6-trinitrophenylazidobenzene (picrylazide) [10–15]. In these studies, it is reported that this material was broken up by two successive exothermic reactions. In the first thermal reaction, the compound is converted to 4,6-dinitrofuroxane by giving a nitrogen molecule at around 120–130 °C. In the second thermal reaction, the furoxane compound formed is reported to be broken off. In the literature recently, the enthalpy of free formation $\left(\Delta H_f^0\right)$ from the picrylazide components was calculated by using theoretical programs and the reaction energy $\left(\Delta H_R^0\right)$ value for the first thermal reaction was theoretically calculated according to the Hess Law. This was followed by measurement of the experimental heat values of the first thermal reaction. The obtained experimental value was then compared with the theoretical value. [15]. Due to the similarity of the picryl and 2,6-dinitro-4-cyanophenyl compounds, similar calculations and measurements were made for the materials prepared in this study. The formation enthalpies were calculated from the elements of the three energetic substances prepared by using the CBS-4M program in the Gaussian package program. Then, the energy released in the first and second thermal reactions of these materials was measured by DSC. The DSC results were corrected by calculating the work done by the gases released as the DSC measurements were made at constant pressure (1).

$$\Delta H^0_{\mathrm{R(corrected)}} = \Delta H^0_{\mathrm{R(measured)}} + \Delta nR\Delta T \quad (1)$$

where $\Delta H^0_{\mathrm{R(measured)}}$ is the heat value measured in the DSC device, Δn is the number of moles of gas substance coming out of the reaction and ΔT is the difference between the temperature and the ambient temperature of the reaction. One of the theoretical difficulties in burst reactions is the difficulty of estimating burst products. Because it is an internal transformation reaction that moves very fast, it is difficult to predict the products precisely. However, TG can be quite helpful in some cases. For example, in this work, the formation of N_2 gas in the first thermal decomposition of 2,6-dinitro-4-cyano-azidobenzene is clearly understood from mass loss. The analytic method that we make the

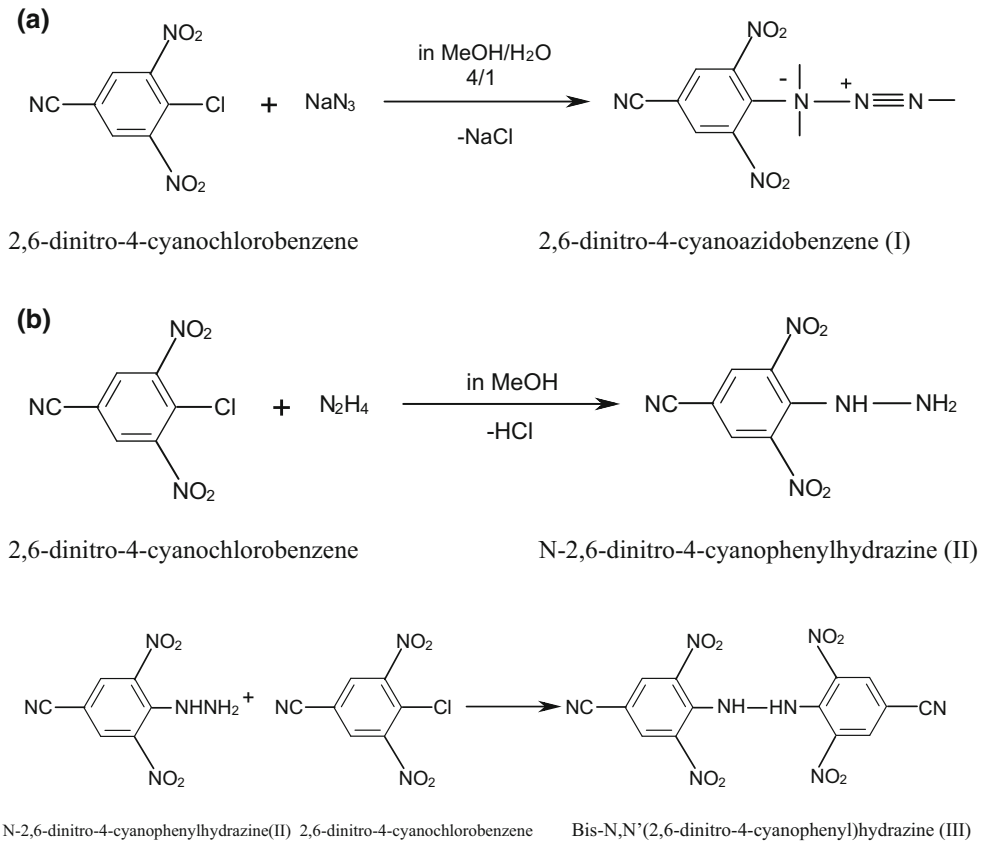

Scheme 1 **a** Preparation of 2,6-dinitro-4-cyano-azidobenzene (I) energetic material and **b** preparation reactions of N-2,6-dinitro-4-cyanophenyl-hydrazine (II) and bis-N,N′(2,6-dinitro-4-cyanophenyl)hydrazine (III)

most use of estimating the products is mass spectrometry. The fragments observed in the mass spectra show clearly which groups of energetic substances have disappeared. In this study, mass fragments were used in predicting the degradation products of the furoxane molecule, especially after the first thermal reaction. Formation enthalpies of the elements of the products may be present in the literature, and if these values are known, the enthalpy of reaction can be calculated according to Hess Law [16] (2).

$$\Delta H^0_{\text{Reaction}} = \sum \Delta H^0_{\text{products}} - \sum \Delta H^0_{\text{reactants}} \quad (2)$$

If the estimated products are unknown, the enthalpy of formation of the elements in this mine can be calculated using CBS-4M.

In addition to these studies, thermal kinetic analysis of thermal reactions of these molecules is carried out with the aid of TG and DSC data. Thermal kinetic analysis was carried out by three different methods: One is the classical Coats–Redfern method (isothermal) applied at a constant heating rate [17–19]. The other two thermokinetic methods are the isoconvertional–nonisothermal methods applied at the different heating rates. These methods are Kissinger–Akahira–Sunose (KAS) and Ozawa–Flynn–Wall (OFW) methods which are very common in the literature [20–27]. As is known, the methods recommended by ICTAC are isoconvertional–nonisothermal methods [22].

As is known, energetic materials have tense molecules. This strain was investigated and added to the study on the effects of five different bacteria and a fungus species, considering that this tension may cause stress in microbial environments. The effects of these three substances on *E. coli, E. facealis, P. aeroginos, B. subtilis* and *S. aureus bacteria*, as well as the effects on *C. albicans* as fungi were investigated. In this study, agar dilution method was used and the minimum inhibitory concentration that killed bacteria and fungi was determined.

Experimental

Apparatus and graphical calculations

The TG–DSC studies were carried out with Shimadzu DTG-60H and Shimadzu DSC-50 apparatus. The thermogravimetric analyses were carried out in Pt pans at a rate of 10 °C min^{-1} under nitrogen atmosphere. The temperature and heat calibrations of both devices were carried out using In and Zn metals. The IR spectra of the ligands and complexes were carried out by the use of Shimadzu brand Infinity model FTIR apparatus equipped with three reflection ATR units, and all IR spectra were recorded at a resolution of 4 cm^{-1}. The mass spectra were obtained by the use of direct inlet (DI) unit of Shimadzu 2010 Plus GCMS apparatus. C, H and N analyses were carried out by Eurovector 3018 CHNS analyzer, and the NMR spectra of the energetic materials were recorded with a Varian brand Mercury model 400-MHz NMR spectrophotometer in d_6-DMSO.

Kinetic analytic studies were carried out using thermogravimetry and differential scanning calorimetry at five different heating rates: 5, 10, 15, 20 and 25 °C min^{-1} for the energetic materials I and III (for 2,6-dinitro-4-cyano-azidobenzene and bis-N,N′(2,6-dinitro-4-cyanophenyl)hydrazine). For N-2,6-dinitro-4-cyanophenyl-hydrazine was used lower heating rate because this material gave an explosion reaction at higher heating rates than 10 °C min^{-1}. For the kinetic analysis of N-2,6-dinitro-4-cyanophenyl-hydrazine were used the data of 0.5, 1.0, 2,5 and 5 °C min^{-1} heating rate.

The kinetic parameters of energetic materials I and III for the KAS and OFW methods were determined using the temperature at the 0.2–0.3–0.4–0.5–0.6–0.7 and 0.8 $g(\alpha)$ values for 5, 10, 15, 20 and 25 °C min^{-1} heating rate from the thermogravimetric or differential scanning calorimetric curves. The activation energy and pre-exponential factor values are calculated with the help of graphical methods using these determined temperature values according to the KAS and OFW methods. The results of Coats–Redfern method were obtained using the temperature at 0.2–0.3–0.4–0.5–0.6–0.7–0.8 $g(\alpha)$ values at the 5, 10, 15, 20 and 25 °C min^{-1} heating rate separately. Furthermore, for energetic material II were used the data at the 0.2–0.4–0.5–0.6–0.7 $g(\alpha)$ values at the heating rate of 0.5, 1.0, 2.5, 5 °C min^{-1}.

For graphical calculations of KAS, OFW and CR methods were used the following formulas according to the literature. For KAS calculations Eq. 3 [24], for OFW Eq. 4 [21] and for CR Eq. 5 [18] were used, respectively.

$$\ln\frac{\beta}{T^2} = \ln\frac{AEa}{Rg(\alpha)} - \frac{Ea}{RT} \quad (3)$$

$$\ln\beta = \ln\frac{0.0048AEa}{Rg(\alpha)} - 1.0516\frac{Ea}{RT} \quad (4)$$

$$\ln\frac{g(\alpha)}{T^2} = \ln\left[\frac{AR}{\beta Ea}\left(1 - \frac{2RT}{Ea}\right)\right] - \frac{Ea}{RT} \quad (5)$$

But in most studies, because the term 1-(2RT/Ea) in parenthetic is approximate ≤ 0.1, the equation is used as below [19].

$$\ln\frac{g(\alpha)}{T^2} = \ln\frac{AR}{\beta Ea} - \frac{Ea}{RT}$$

In these equations, β term in equation shows heating speed as °C min^{-1}, R term universal gas constant, E_a term thermal disintegration activation energy, A term Arrhenius

pre-exponential factor, T temperature as K. $g(\alpha)$ term determines fractional completed fraction of thermal fracture reaction. These equations were written as accepting reaction order $n = 1$ and considering realized as mentioned above. In all three methods, $\ln\beta$, $\ln[\beta/T^2]$ and $\ln[g(\alpha)/T^2]$ are plotted against $1/T$ values; consequently, E_a values and A values were calculated using slope and intercept, respectively, from the lines obtained.

Based on E_a and A values, some thermodynamic parameters in thermal reactions can be calculated easily. In most references, with the help of pre-exponential factor, the entropy change in thermal reaction can be calculated with

$$\Delta S = 2.303\left[\log\frac{Ah}{kT}\right]R \tag{6}$$

equation as approximately. Beside this, as per the first rule of the thermodynamic, easily

$$\Delta H = Ea - R\Delta T \tag{7}$$

equation can be written, and as per the Gibbs Free energy equation, from Eq. 8, the Gibbs Free energy can be calculated [19].

$$\Delta G = \Delta H - T\Delta S \tag{8}$$

Theoretical calculation

The enthalpies (H) and free energies (G) were calculated using the CBS-4M method included in the Gaussian G09W (revision D.01) software package [28–30]. The CBS-4M begins with a HF/3-21G(d) in order to structure optimization and zero-point energy calculations. It then uses a large basis set SCF and MP2/6-31+G calculations as a base anergy and to correct the energy through the second order, respectively. A MP4(SDQ)/6-31+(d,p) calculation is used to approximate higher-order contributions [31–33].

Explosion products were estimated in accordance with the literature data and using mass spectra [34]. The formation enthalpies of these estimated products were determined from the literature or calculated using the same methods. Then, using these theoretical values according to the Hess Law, the enthalpies of the first and second thermal reactions were calculated.

$$\Delta H^0_{\text{Reaction}} = \sum \Delta H^0_{\text{products}} - \sum \Delta H^0_{\text{reactants}} \tag{2}$$

Here, $\Delta H^0_{\text{Reaction}}$ is the theoretical reaction enthalpy, $\Delta H^0_{\text{products}}$ is the formation enthalpy of the products estimated or calculated and $\Delta H^0_{\text{reactants}}$ is the calculated formation enthalpy of energetic material.

Determination of biological activity

The three energetic materials were also tested for their antimicrobial activity. 3 g (−) (*Escherichia coli*, *Pseudomonas aeruginosa, Enterococcus faecalis)* and 2 grams (+) (*Bacillus subtilis*, *Staphylococcus aureus*) bacterial strains were used for antibacterial assay [35, 36]. We also tested the complexes against *C. albicans* as a pathogenic fungal strain. For bacterial strains, Muller–Hinton agar (HMA) was used for bacterial growth and Sabouraud dextrose agar (SDA) for *C. albicans* [37]. Minimum inhibitory concentrations for each microbial strain were calculated by agar dilution method. 24-h fresh cultures were used to inoculate the test agars, which were also prepared with HMA-containing chemical agent going to be tested. 10-μL bacterial suspension (10^6 Cfu mL^{-1} according to McFarland turbidity standard) of each strain was dropped on to the agar plates.

Concentrations of chemicals for MIC assay were in the range of 512.0–4.0 mg dm^{-3}. The MIC was read after 24 h of incubation at 37 °C and 24 h for *C. albicans*. Control antimicrobial tests of solutions were prepared in DMSO. Double serial dilutions were also prepared in the same solvent. The inoculated plates were incubated for 24 h at 36 °C for bacteria and for 48 h at same temperature for the yeast. Positive controls (amoxicillin) were used to control the sensitivity of the tested bacteria, and amphotericin B was used as controls against the tested fungi.

Preparation of energetic materials

Preparation of 2,6-dinitro-4-cyano-azidobenzene (**I**): 2,6-dinitro-cyano-chlorobenzene (0.01 mol, 2.28 g) was dissolved in 50 mL MeOH/H_2O mixture (80%:20%, v/v) under stirring and heating. The solution was heated up to 50 °C, and to this solution was added a solution of sodium azide (0.01 mol, 0.65 g) in 30 mL MeOH/H_2O/acetone (40%:30%:30%, v/v/v) mixture. The resulting mixture was refluxed for 2 h and after this period was set aside. The precipitated yellow crystals were filtered and dried in air and recrystallized from MeOH. Yield %: 60–65. Melting point: 116–117 (from TG)

Elemental Analysis For $C_7H_2N_6O_4$:

Anal. Calcd. %: C: 35.91; H: 0.86; N: 35.88.

Found %: C: 35.47; H: 1.24; N: 36.49.

Important IR data (cm^{-1}): $\nu_{C-H(Ar)}$: 3086, ν_{CN}: 2243, ν_{NNN}:2146–2127, $\nu_{C=N}$: 1614, $\nu_{C=C(ring)}$: 1532, $\nu_{N=O}$:1321–1350, $\delta_{C-H\ (Ar)}$: 752.

m/z: 234 (molecular peak), 206, 176, 160, 146,130, 118, 100 (base peak), 87, 75.

^1H NMR data in d_6-DMSO(δ, ppm): 8.915 (s)

^{13}C NMR data in d_6-DMSO (δ, ppm): 143.95, 133.72, 132.96, 115.32, 107.66

Preparation of N-2,6-dinitro-4-cyanophenyl-hydrazine (**II**): 2,6-dinitro-cyano-chlorobenzene (0.01 mol, 2.28 g) was dissolved in 50 mL MeOH under stirring and heating. This solution was heated up to boiling point and added a solution of hydrazine hydrate (0.015 mol, 0.75 g) in 20 mL MeOH. The final solution was refluxed 15–20 min and was left aside. The resulting dark brown crystals were filtered after 3–4 h and dried in air and recrystallized from MeOH. Yield: %70–75. Melting point is not observed.

Elemental Analysis For $C_7H_5N_5O_4$:

Anal. Calcd. %: C: 37.68; H: 2.26; N: 31.37.

Found %: C: 37.29; H: 1.96; N: 30.59.

Important IR data (cm^{-1}): ν_{N-H}:3331–3321–3238, $\nu_{C-H(Ar)}$: 3111, ν_{CN}: 2247, $\nu_{C=N}$: 1641–1625, $\nu_{C=C(ring)}$: 1568-1525, $\nu_{N=O}$:1367–1265, $\delta_{C-H\ (Ar)}$: 734.

m/z: 223 (molecular peak), 205, 176, 147,131, 100 (base peak), 88, 76.

^1H NMR data in d_6-DMSO(δ, ppm): 9.808 (s, broad), 8.554 (s), 4.865 (s, broad).

^{13}C NMR data in d_6-DMSO (δ, ppm): 142.49, 134.07, 132.32, 114.67, 95.01.

Preparation of bis- N,N′(2,6-dinitro-4-cyanophenyl)hydrazine (**III**): 2,6-dinitro-cyano-chlorobenzene (0.01 mol, 2.28 g) was dissolved in 50 mL MeOH under stirring and heating. To this solution was added a solution of hydrazine hydrate (0.0048 mol, 0.24 g) in 20 mL MeOH. The final solution was heated 15–20 min and was left aside. 5–6 h after were filtered the formed orange crystals and dried in air and recrystallized in MeOH/MeCN. Yield: %80–85. Melting point: 136–137 °C (from TG)

Elemental Analysis For $C_{14}H_6N_8O_8$:

Anal. Calcd. %: C: 40.60; H: 1.46; N: 27.04.

Found %: C: 39.81; H: 1.34; N: 26.58.

Important IR data (cm^{-1}): ν_{N-H}:3321–3240, $\nu_{C-H(Ar)}$: 3109-3086, ν_{CN}: 2245, $\nu_{C=N}$: 1641–1620, $\nu_{C=C(ring)}$: 1570–1520, $\nu_{N=O}$:1415–1354, $\delta_{C-H\ (Ar)}$: 725.

m/z: 366,223, 206, 178, 147, 131, 100 (base peak), 88, 76, (molecular peak was not observed).

^1H NMR data in d_6-DMSO (δ, ppm): 9.977 (s, broad), 8.948 (s).

^{13}C NMR data in d_6-DMSO (δ, ppm): 145.29, 133.73, 133.12, 117.43, 104.02.

Results and discussion

The curves obtained from the prepared energetic materials by using a heating rate of 10 °C min^{-1} and by using TG method are shown in Fig. 1a, and DTA curves at same heating rate are given in Fig. 1b.

As shown in Fig. 1a, 2,6-dinitro-4-cyano-azidobenzene (I) gives two successive exothermal reactions. In contrast, in the case of the N-2,6-dinitro-4-cyanophenyl-hydrazine (II) and bis-N,N′(2,6-dinitro-4-cyanophenyl)hydrazine (III) when we lower the heating rate, as it can be seen from the DSC curves, two successive thermal reactions occur in (II) and (III). In Fig. 2, they are observed at (0.5) and (1.0) C min^{-1}. TG–DTA curves are obtained at heating rates.

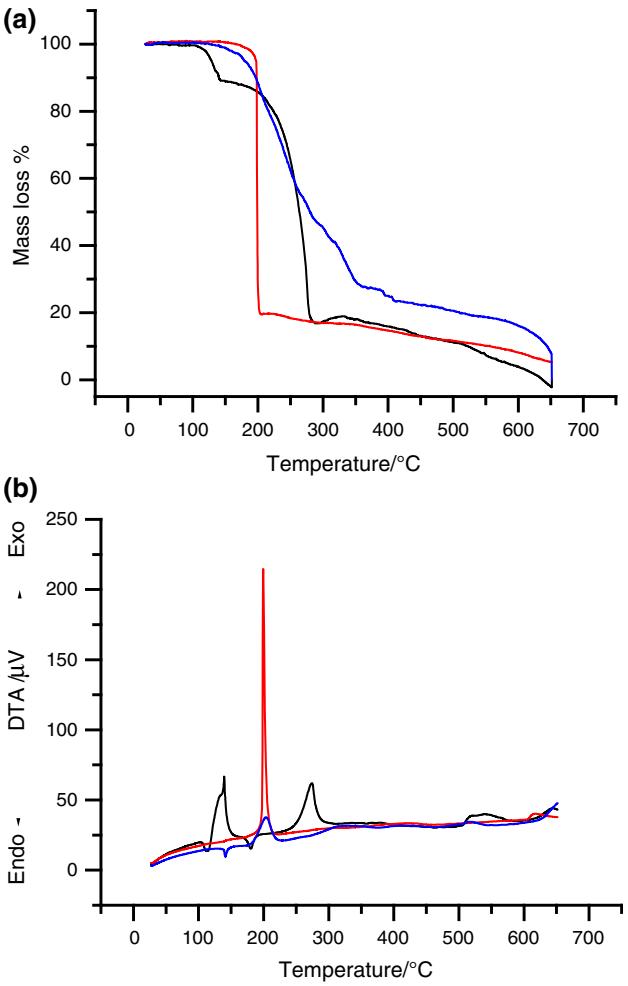

Fig. 1 **a** TG curves obtained from the prepared energetic materials by using a heating rate of 10 °C min^{-1}. Black: 2,6-dinitro-4-cyano-azidobenzene (I), red: N-2,6-dinitro-4-cyanophenyl-hydrazine (II), blue: bis-N,N′(2,6-dinitro-4-cyanophenyl)hydrazine (III). **b** Prepared energetic substances 10 °C min^{-1}. DTA curves obtained at the heating rate. Black: 2,6-dinitro-4-cyano-azidobenzene (I), red: N-2,6-dinitro-4-cyanophenyl-hydrazine (II), blue: bis-N,N′(2,6-dinitro-4-cyanophenyl)hydrazine (III)

In Fig. 2, it is seen that the energetic substance is broken down by two successive thermal reactions when the heating rate is low. When temperature is 5 °C min^{-1} or higher, the reaction appears to be a single explosion reaction. At heating rate 5.0 °C min^{-1} when the first thermal reaction starts, the explosion-causing gas is removed from the atmosphere while the gas is removed and the temperature is decreased very shortly. However, at heating rates of 0.5–2 °C min^{-1}, two successive reactions at heating rates can be clearly selected. The same situation is seen in DSC curves. In Fig. 3,

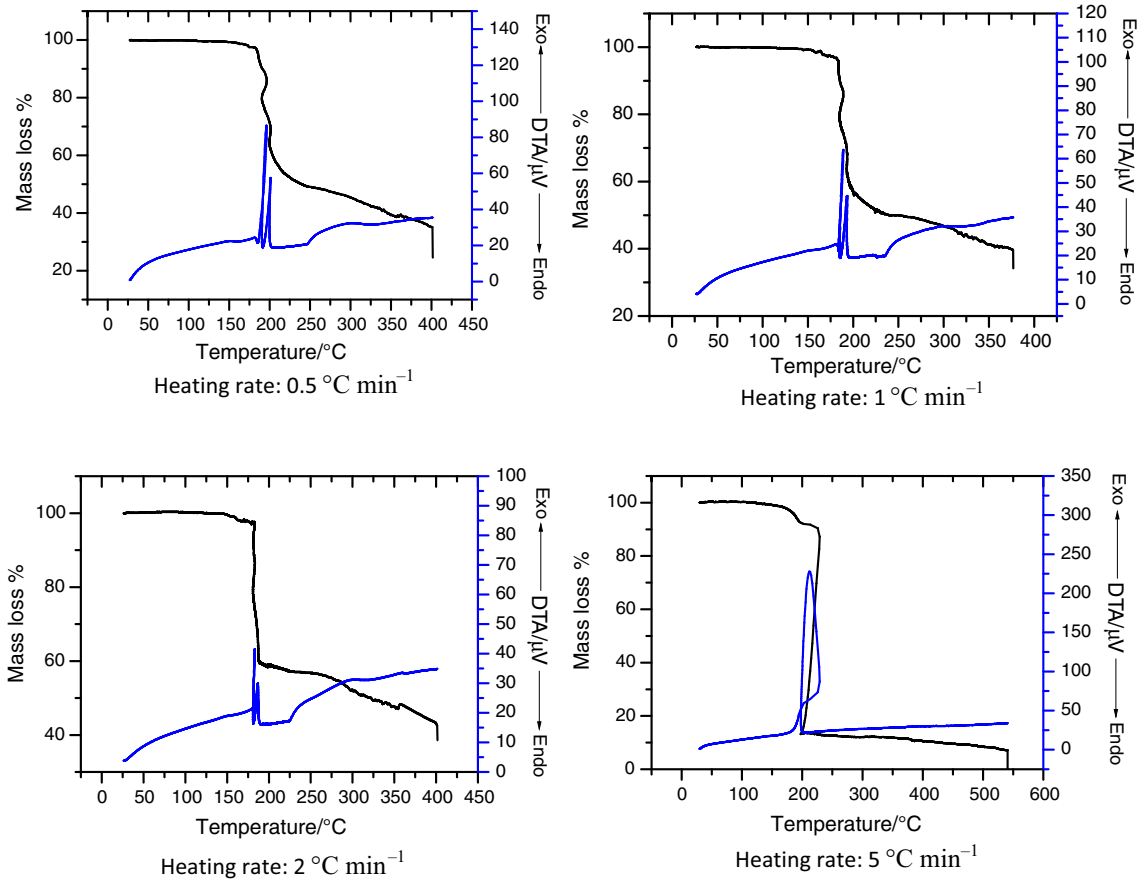

Fig. 2 TG–DTA curves of N-2,6-dinitro-4-cyanophenyl-hydrazine at 0.5–5 °C min^{-1} heating rates

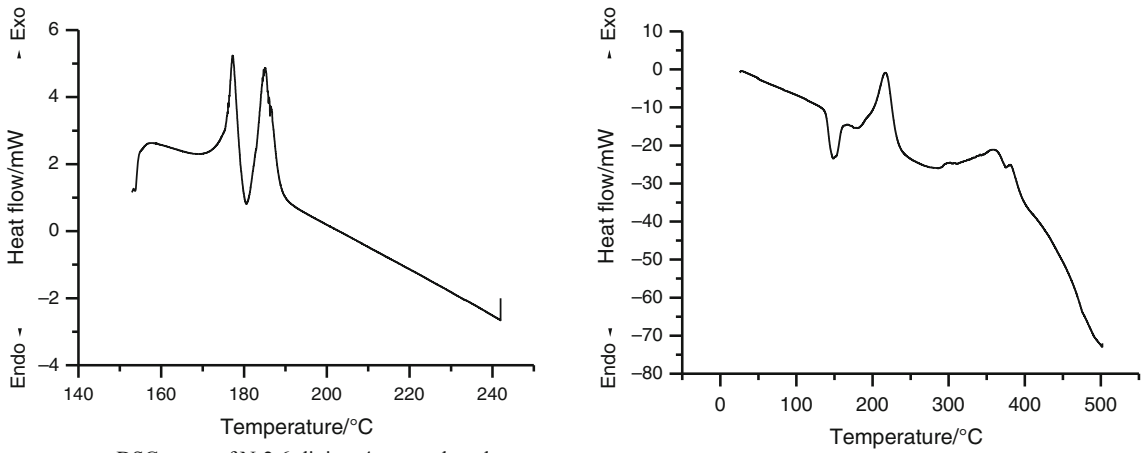

Fig. 3 DSC curves of N-2,6-dinitro-4-cyanophenyl-hydrazine (II) and bis-N,N′(2,6-dinitro-4-cyanophenyl)hydrazine (III) energetic substances. The thermoanalytical data found in TG and DSC studies of these materials are shown in Table 1

DSC curves of N-2,6-dinitro-4-cyanophenyl-hydrazine (II) and bis-N,N′(2,6-dinitro-4-cyanophenyl)hydrazine (III) are given. There are two thermal reactions on both sides, and the initial and final temperatures of these reactions can be selected. In the DSC curve of N-2,6-dinitro-4-cyanophenyl-hydrazine (II) are selected clearly two exothermic peaks. In

Table 1 Thermoanalytical data of the prepared energetic materials

Energetic material	First thermal reaction				Second thermal reaction			
	Melting point (peak of the fusion curve/ °C)	Temperature range/°C	Calculated mass loss/ %	Measured mass loss/ %	Melting point (peak of the fusion curve/ °C)	Temperature range/°C	Calculated mass loss/ %	Measured mass loss/%
I								
5 °C min^{-1}	109.63 TG	109.63-144.34/DTA peak:128.48 TG	11.96	11.31	179.00 TG	195.39-858.26/DTA peak:258.09 TG	59.83	64.62
10 °C min^{-1}	114.46 TG	109.63-144.34/DTA peak:128.48 TG		11.606	180.52 TG	211.92-313.08/DTA peak:274.08 TG		66.96
15 °C min^{-1}	115.56 TG	109.63-144.34/DTA peak:128.48 TG		11.246	182.64 TG	219.08-327.47/DTA peak:286.72 TG		63.34
20 °C min^{-1}	115.73 TG	109.63-144.34/DTA peak:128.48 TG		10.971	184.00 TG	219.62-329.61/DTA peak:293.80 TG		68.54
25 °C min^{-1}	120.13 TG	109.63-144.34/DTA peak:128.48 TG		11.909 Average: 11.41±0.36	Not measured	229.22-329.92/DTA peak:302.24 TG		65.85 Average: 65.82±2.21
II								
0.5 °C min^{-1}	157.84 DSC	173.76-182.63/ peak:179.28 DSC	7.62	8.63	–	182.63-192.27/ peak:186.91 DSC	62.33	56.27
1 °C min^{-1}	156.93 DSC	173.56-183.64/ peak:182.02 DSC		9.05	–	185.02-196.18/ peak:190.37 DSC		53.79
2.5 °C min^{-1}	158.28 DSC	179.25-185.64/ peak:182.57 DSC		8.48	–	189.25-199.51/ peak:194.25 DSC		53.93
5 °C min^{-1}	159.79 DSC	182.91-204.44/ peak:200.83 DSC		8.11 Average: 8.57±0.39	–	204.44-218.22/ peak:212.39 DSC		89.82 Average: 63.45±19.23
III								
5 °C min^{-1}	134.97 TG	153.46-191.17/DTA peak:189.97 TG	0.48	14.053	179.00 TG	195.39-858.26/DTA peak:258.09 TG	59.83	58.98
10 °C min^{-1}	129.62 TG	170.51-220.37/DTA peak:205.89 TG		15.094	180.52 TG	211.92-313.08/DTA peak:274.08 TG		66.96

Table 1 continued

Energetic material	First thermal reaction				Second thermal reaction			
	Melting point (peak of the fusion curve/°C)	Temperature range/°C	Calculated mass loss/%	Measured mass loss/%	Melting point (peak of the fusion curve/°C)	Temperature range/°C	Calculated mass loss/%	Measured mass loss/%
15 °C min^{-1}	140.27	171.71-211.79/DTA peak:207.04		13.623	182.64	219.08-327.47/DTA peak:286.72		63.34
	TG	TG			TG	TG		
20 °C min^{-1}	141.51	177.08-228.43/DTA peak:217.51		15.875	184.00	219.62-329.61/DTA peak:293.80		68.54
	TG	TG			TG	TG		
25 °C min^{-1}	140.40	180.32-235.67/DTA peak:222.90		14.168	Not measured	229.22-329.92/DTA peak:302.24		65.85
	TG	TG		Average 14.56±1.06		TG		Average: 65.82±2.21

the DSC curve of N-2,6-dinitro-4-cyanophenyl-hydrazine (II), there are two clearly selected exothermic peaks. However, in other DSC curves there are one endothermic and two exothermic peaks. This endothermic signal that is observed at 141.7 °C is the melting point of bis-N,N′(2,6-dinitro-4-cyanophenyl)hydrazine.

As shown in Table 1, in the energetic material no. I, mass loss in the first thermal reaction attributed to a nitrogen molecule. This is clearly seen. Nitrogen loss is not the case in energetic materials no. II and III. Mass spectra were used for the first and second decay products of these materials. If we look at the m/z values given in the Experimental part, the signals outside the molecular peak are quite similar. Almost the same fragments occur in three energetic substances. m/z = 205 or 206,176, 147,130 or 131 and 100 signals are common. The m/z = 100 signal in the mass spectrum of all three materials is the basic peak. Only the bis-N,N′(2,6-dinitro-4-cyanophenyl)hydrazine molecular peak III is not observed, but instead the 368 signal is present. Possible explanations of these fragments are given in Scheme 2. The thermal degradation of 2,4,6-trinitroazidobenzene (picrylchloride) has been described in detail in the literature [11, 13, 15]. Picrylchloride is converted to 4,6-dinitrofuroxane by giving an N_2 molecule at around 120 °C. This furoxane compound is then decomposed by an exothermic reaction at 170–200 °C.

Scheme 3 estimates of the m/z values of the observed fragments in the mass spectrum of the 2,6-dinitro-4-cyano-azidobenzene (I) material are given. However, if we look at the m/z values of other energetic substances, 206,176, 147,100 were observed in three items. The m/z = 100 signal appears as the base peak in the mass spectra of the three materials. In this case, the formation of furoxane is likely to be the same in these energetic substances, and the first thermal reactions of the three energetic substances prepared are given, as shown in Scheme 3.

The intermediate product 4-nitro-6-cyano-1-oxyfuroxane, which is formed as a result of the first thermal reaction, is decomposed by thermal reaction. Using the literature, the products that come into play in this fragmentation reaction are as follows in Scheme 4.

If these reaction products are correct, the energy released in these reactions must be the same or comparable to the theoretically calculated energies. The enthalpy of free formation from the elements of the energetic materials prepared in the first thermal reaction and the intermediate 4-nitro-6-cyano-1-oxyfuroxane was theoretically calculated. The enthalpy of formation of the elements H_2 (g) and N_2 (g) is zero, and the formation enthalpies of the $NH_{3(g)}$ and the entrained substances evolved in the second reaction can be found in the literature [34].If the reaction enthalpy is calculated according to the Hess Law (Eq. 2), the situation given in Table 2 arises.

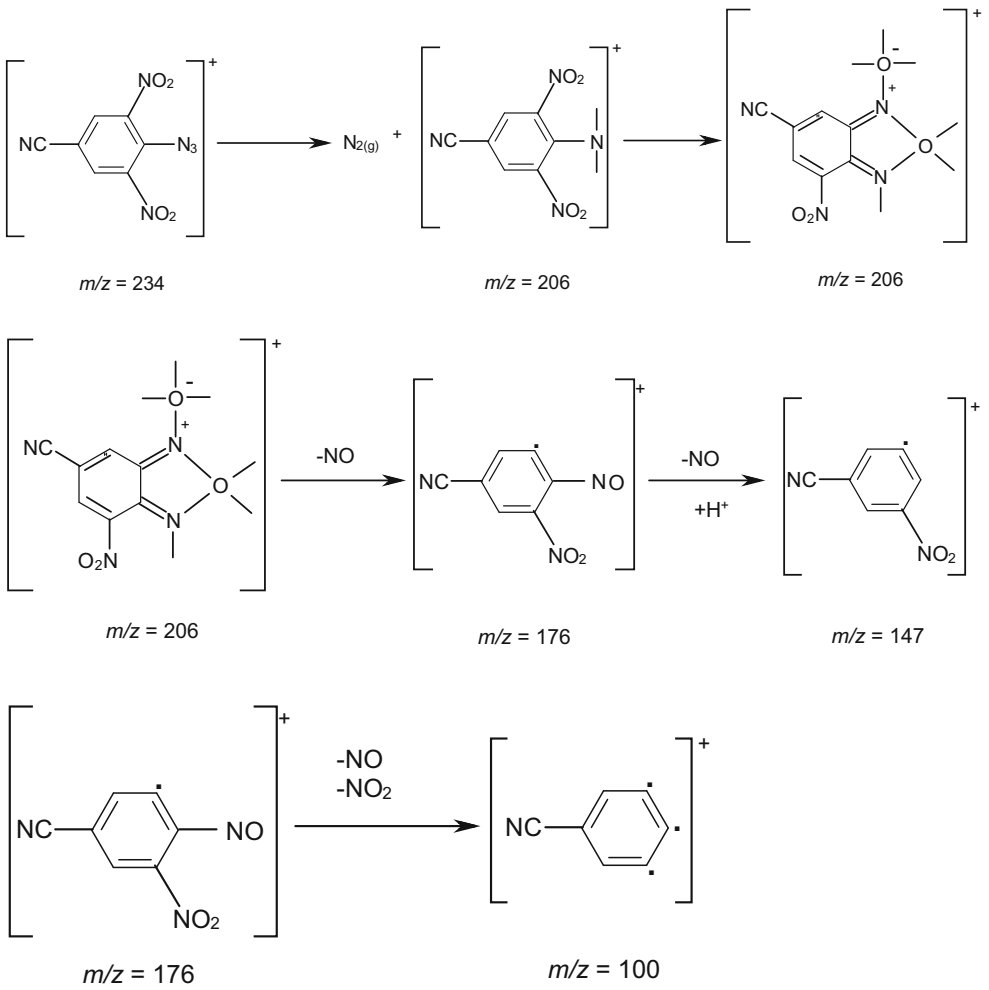

Scheme 2 Six fragmentations observed in the mass spectrum

$$\Delta H_{\mathrm{R}}^{0} = \sum \Delta H_{\mathrm{products}}^{0} - \sum \Delta H_{\mathrm{reactants}}^{0} \quad (2)$$

The theoretical and experimental values given in Table 2 also indicate the success of the CBS-4M algorithm in energy calculation.

Thermal kinetic analysis was calculated using TG and DSC data for the three energetic substances prepared. As noted above, thermal kinetic analysis was performed using an isothermal method (CR) and two different isoconversional–nonisothermal methods (KAS and OFW). The graphs of KAS, OFW and CR obtained in the thermal reactions 1 and 2 of 2,6-dinitro-4-cyano-azidobenzene (I) are given in Fig. 4a–f, respectively.

Activation energies (E_a) and the Arrhenius pre-exponential factors (A) of three energetic materials in the first and second thermal reactions can be seen in Table 3. Other thermodynamic parameters (AH^0, ΔS and ΔG^0) found using these values are given in Table 4.

For the 2,6-dinitro-4-cyano-azidobenzene (I), the initial and final temperatures of the two thermal reactions are clearly observed in the TG curve. In this article, g (α) and T values of two thermal reactions can easily be determined at heating rates of 5.0–10.0–15.0–20.0–25.0 °C min^{-1} In contrast, in N-2,6-dinitro-4-cyanophenyl-hydrazine (II) at heating rates higher than 5 °C min^{-1}, there is only one reaction instead two thermal reactions. Only at low heating rates, two reactions can be distinguished. However, even at low speeds, the initial and final temperatures of the first and second thermal reactions are clearly defined. For this reason, the starting and ending temperatures of the first and second thermal reactions of this material were determined from the DSC curves at heating rates of g (α) values of 0.5–1.0–2.5 and 5.0 °C min^{-1}, as shown in Fig. 5. Bis-N, N ′ G (α) and T values are obtained from TG curves, and thermal response g (α) and T values in the first thermal reaction of the 6-dinitro-4-cyanophenyl from DSC curve are 5.0–10.0–15.0–20.0–25.0 °C min^{-1}, respectively.

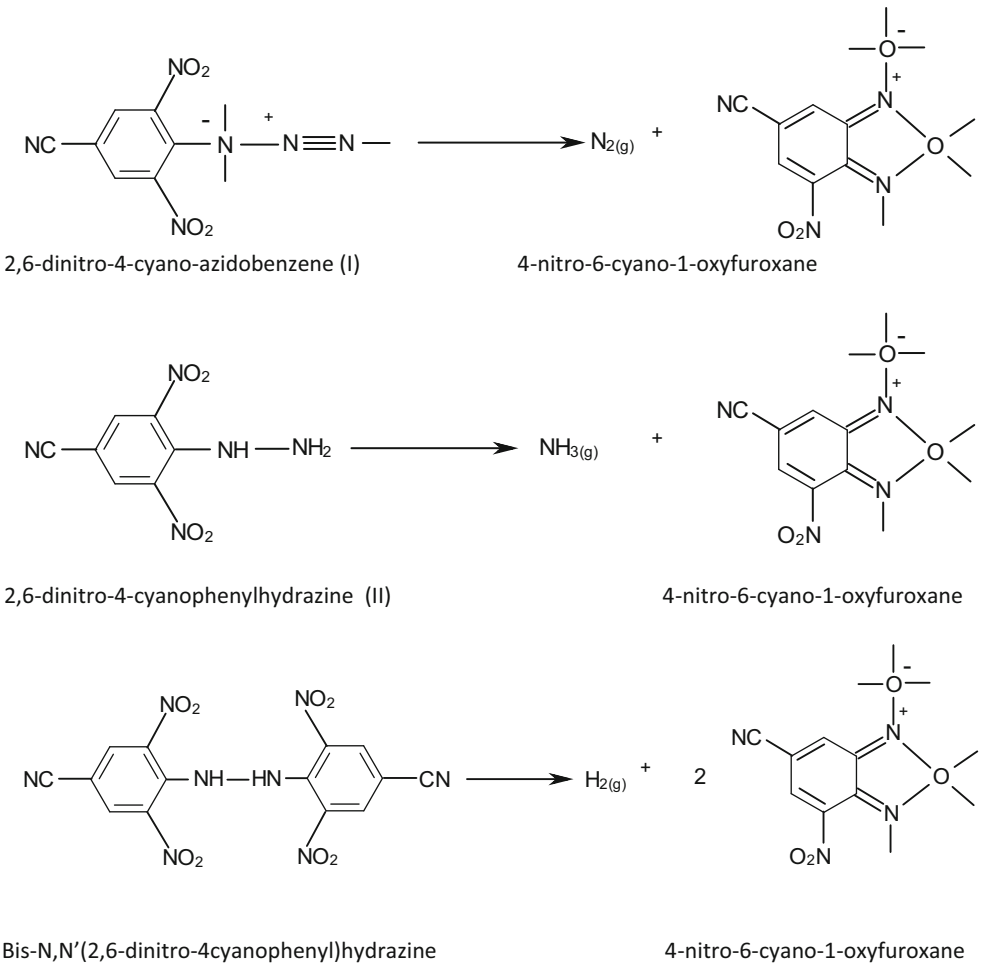

Scheme 3 First thermal reactions of prepared energetic substances and their products

Scheme 4 Degradation products in the second thermal reaction of 4-nitro-6-cyano-1-oxyfuroxane intermediate products

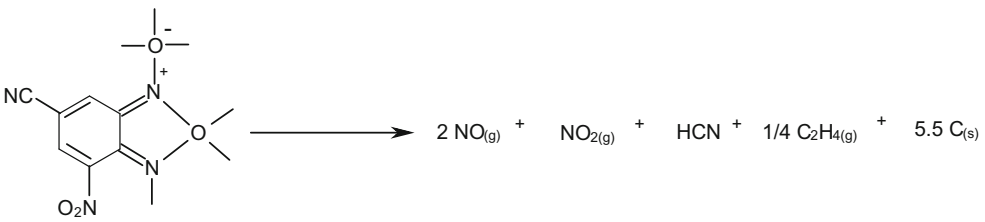

As shown in Table 3, the KAS and OFW methods are similar to each other, so the values of Ea are very close to each other. If T and g (α) values are clearly determined, then E_a values are close. Only the N-2,6-dinitro-4-cyano-phenyl-hydrazine compound was found to have high activation energy values for the first and second thermal reactions in the calculation of the CR method. The CR method is an isothermal method, and therefore, it is expected to have different results from the KAS and OFW methods. The same situation can not be said for Arrhenius pre-exponential factor values. The values of A calculated as the result of KAS, OFW and CR equations are not comparable to each other. Although there are similar methods, the results of KAS and OFW methods are very different from each other. They are incomparable values. However, it is clear that this difference is due to the calculation method. In obtaining Ea values in all three methods, the result of multiplying the slope value by R value is obtained. However, there are three different methods for calculating A value, which cause difference in results. However, A values do not lead to much difference in the calculation of thermodynamic parameters. The value calculated from A is the entropy value (S), and this value is used in the Gibbs free energy calculation. Equation 4

Table 2 Comperative calculated and measured ΔH_R^0 values

Energetic material		Calculated ΔH_f^0/ kJ mol^{-1}	Products	Calculated ΔH_R^0/ kJ mol^{-1}	Measured heat in DSC/kJ mol^{-1}	Improved heat value (with ΔnRT improvement)/ kJ mol^{-1}
2,6-dinitro-4-cyano-azidobenzene (I)	1. Thermal reaction	321.09	$N_{2(g)}$ and 4-nitro-6-cyano-1-oxyfuroxane	−114.17	−112.26 ± 4.44	−113.34 ± 4.44
	2. Thermal reaction		$2NO_{(g)}$, $NO_{2(g)}$, $HCN_{(g)}$, ¼ $C_2H_{4(g)}$, 5,.5 $C_{(s)}$	−118.58	−105.50 ± 18.45	−114.97 ± 18.45
2,6-dinitro-4-cyanophenyl-hydrazine (II)	1. Thermal reaction	594.69	$NH_{3(g)}$ and 4-nitro-6-cyano-1-oxyfuroxane	−113.49	−108.16 ± 13.73	−109.84 ± 13.73
	2. Thermal reaction		$2NO_{(g)}$, $NO_{2(g)}$, $HCN_{(g)}$, ¼ $C_2H_{4(g)}$, 5,.5 $C_{(s)}$	−118.58	−103.31 ± 3.08	−110.23 ± 3.08
Bis-N,N′(2,6-dinitro-4-cyanophenyl)hydrazine (III)	1. Thermal reaction	562.98	$H_{2(g)}$ and 4-nitro-6-cyano-1-oxyfuroxane	−82.46	−78.69 ± 4.34	−80.17 ± 4.34
	2. Thermal reaction		$2NO_{(g)}$, $NO_{2(g)}$, $HCN_{(g)}$, ¼ $C_2H_{4(g)}$, 5,.5 $C_{(s)}$	−118.58	−122.74 ± 12.09	−134.83 ± 12.09
4-nitro-6-cyano-1-oxyfuroxane (intermediate)		480.52	$2NO_{(g)}$, $NO_{2(g)}$, $HCN_{(g)}$, ¼ $C_2H_{4(g)}$, 5,.5 $C_{(s)}$	−118.58		

requires that the calculated S values are not very different when the A values are very different. Here, the calculated ΔH values given in Table 4 and the ΔH_R^0 values given in Table 2 are different from each other. The values given in Table 2 are energy values that are released in the thermal reaction of the energetic material. As shown in Table 2, the free enthalpy values calculated by CBS-4M theoretically are positive values, but the reaction enthalpies are found to be negative (exothermic). The ΔH values and other thermodynamic values given in Table 3 are only the values in the activation of the energetic substance in thermal reactions.

In this study, the estimations of the products of thermal reactions are probably correct. Similar results have been found in previous studies [12, 15, 38, 39]. The experimental and theoretical reaction enthalpies are close and comparable. Here is the success of the CBS-4M program. Free formation from the elements of energetic substances is a very successful application in the calculation of enthalpy. The reaction products, which should be interpreted in the calculation of the enthalpy of the reaction, do not conform to the oxygen balance (Ω) rules [40, 41]. In the burst reaction of the energetic substance, the molecule indicates that all nitrogen atoms are converted to N_2 (g). N_2 (g) formation is not seen in the reactions given above. The formation of NO (g) and NO_2 (g) gases is suggested. Furoxane formation is inevitable if nitrogen groups are attached to nitro groups in the ortho position of energetic substance molecules. This is due to the fact that the energetic substance is broken down in two stages, and the reaction products do not conform to the Ω rules.

As it is known, energetic substance molecules are tense molecules, and this tension is likely to cause stress in biological tissues. Biological activities against five different bacteria and a fungus of energetic substances prepared in this way were measured. Bacteria used were *E. coli, E. facealis, P. aeroginosa, B. subtilis, S. aureus.* The purpose of this work is to determine the stress effect of energetic substance molecules on microorganisms in the environment. The goal is to understand the biological reverberation of molecular tension. The results are given in Table 5.

As shown in Table 5, all three materials have antimicrobial effects. The energetic substance no I containing the azide group is effective in all bacterial strains and in *C. albicans* and has the highest antimicrobial activity. This material has a minimum inhibitory concentration (MIC) value of 8 mg dm^{-3} for *B. subtilis* and 4 mg dm^{-3} for *C. albicans*. Energetic substances II and III have less antimicrobial activity. When these two energetic materials were compared, it was found that bis-N,N′(2,6-dinitro-4-cyanophenyl)hydrazine material no (III) is more effective on *C. Albicans*. It performed more inhibition compared to

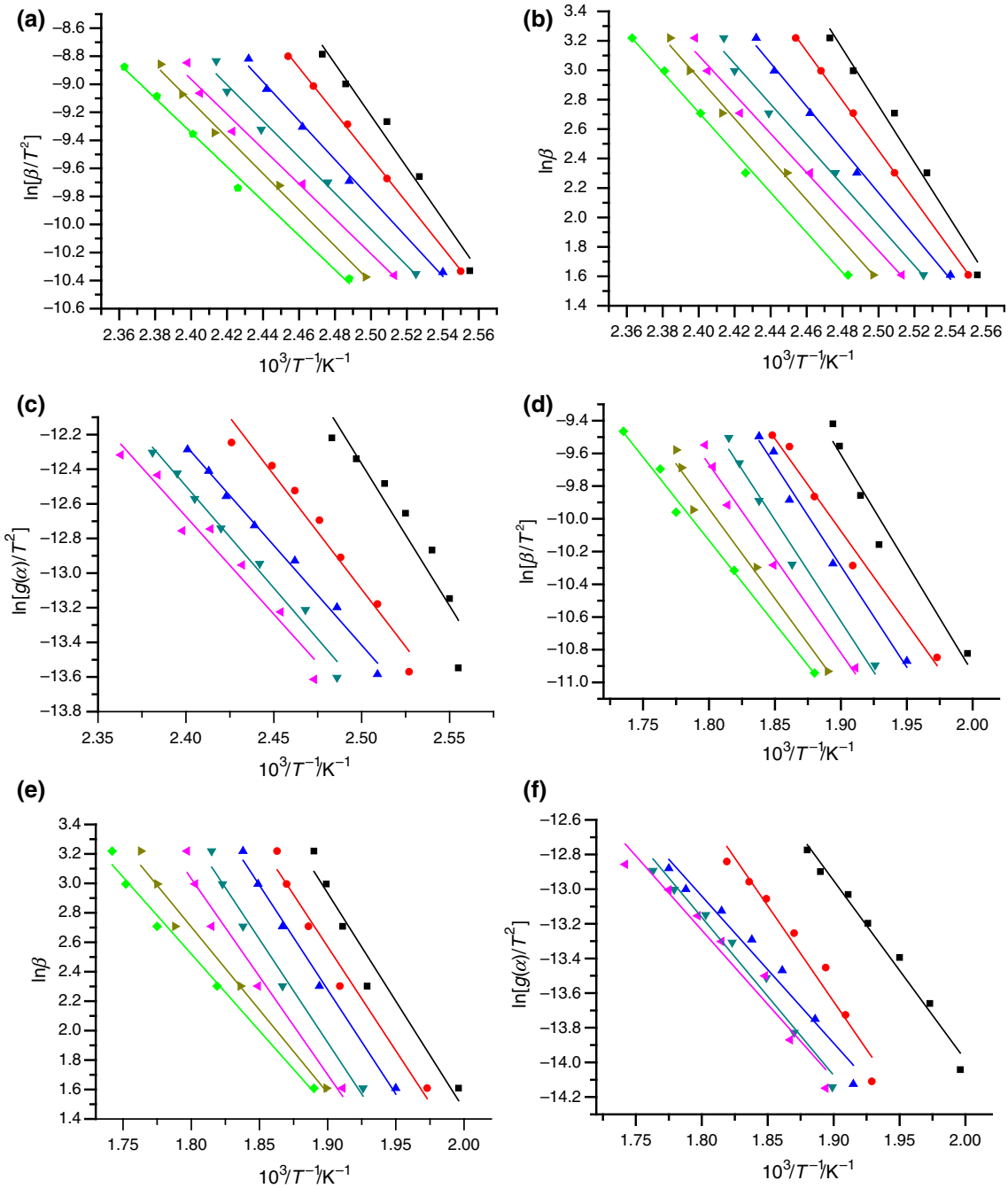

Fig. 4 **a** 2,6-Dinitro-4-cyano-azidobenzene (I) KAS graphics for 1. thermal reaction, black: $g(\alpha) = 0.2$, red: $g(\alpha) = 0.3$, blue: $g(\alpha) = 0.4$, dark green: $g(\alpha) = 0.5$, pink: $g(\alpha) = 0.6$, dark yellow: $g(\alpha) = 0.7$, light green: $g(\alpha) = 0.8$. **b** 2,6-Dinitro-4-cyano-azidobenzene (I) OFW graphics for 1. thermal reaction, black: $g(\alpha) = 0.2$, red: $g(\alpha) = 0.3$, blue: $g(\alpha) = 0.4$, dark green: $g(\alpha) = 0.5$, pink: $g(\alpha) = 0.6$, dark yellow: $g(\alpha) = 0.7$, light green: $g(\alpha) = 0.8$. **c** 2,6-Dinitro-4-cyano-azidobenzene (I) CR graphics for 1. thermal reaction, black: $\beta = 5$, red: $\beta = 10$, blue: $\beta = 15$, dark green: $\beta = 20$, pink: $\beta = 25$ °C.min^{-1} heating rate. **d** 2,6-Dinitro-4-cyano-azidobenzene (I) KAS graphics for 2. thermal reaction, black: $g(\alpha) = 0.2$, red: $g(\alpha) = 0.3$, blue: $g(\alpha) = 0.4$, dark green: $g(\alpha) = 0.5$, pink: $g(\alpha) = 0.6$, dark yellow: $g(\alpha) = 0.7$, light green: $g(\alpha) = 0.8$. **e** 2,6-Dinitro-4-cyano-azidobenzene (I) OFW graphics for 2. thermal reaction, black: $g(\alpha) = 0.2$, red: $g(\alpha) = 0.3$, blue: $g(\alpha) = 0.4$, dark green: $g(\alpha) = 0.5$, pink: $g(\alpha) = 0.6$, dark yellow: $g(\alpha) = 0.7$, light green: $g(\alpha) = 0.8$. **f** 2,6-Dinitro-4-cyano-azidobenzene (I) CR graphics for 2. thermal reaction, black: $\beta = 5$, red: $\beta = 10$, blue: $\beta = 15$, dark green: $\beta = 20$, pink: $\beta = 25$ °C.min^{-1} heating rate

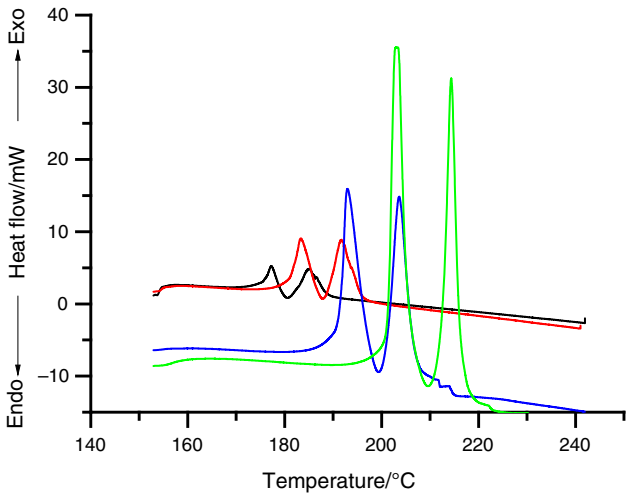

Fig. 5 DSC curves of N-2,6-dinitro-4-cyanophenyl-hydrazine (II) at 0.5–1.0–2.5 and 5.0 °C min^{-1} heating rate

N-2,6-dinitro-4-cyanophenyl-hydrazine. In Table 3, theoretical enthalpies of formation of these energetic substances from their elements are given. Calculated values for I, II and III are 594.69, 321.09 and 562.98 kJ mol^{-1}, respectively. All formation enthalpies were found to be positive. The magnitudes of these values indicate the approximate stability of these compounds. The more positive the enthalpy of free formation from the elements is, the more complex it is. The values given in Table 5 correspond to this idea in reality. The most tense compound is no I, 2,6-dinitro-4-cyanophenylazidobenzene and has the highest antimicrobial activity. The compound, N (2,6-dinitro-4-cyanophenyl)hydrazine (III), which is in the order of 2 in the sequence, is the compound with the second highest antimicrobial activity. N-2,6-dinitro-4-cyanophenyl-hydrazine which is no I is the least tense one and has the lowest antimicrobial activity. It should be noted here

Table 3 Graphical calculated activation energy and Arrhenius pre-exponential factor values (the method used to calculate $g(\alpha)$ and T values (TG or DSC) is given in the table)

Energetic materials	Measuring and calculation methods							
	KAS				OFW			
	First thermal reaction		Second thermal reaction		First thermal reaction		Second thermal reaction	
	E_a/kJ mol^{-1}	A/min^{-1}	E_a/kJ mol^{-1}	A/min^{-1}	E_a/kJ mol^{-1}	A/min^{-1}	E_a/kJ mol^{-1}	A/min^{-1}
I	117.43 ± 1.18	1.07×10^5	96.96 ± 1.05	5.71×10^{10}	123.11 ± 1.26	2.88×10^{13}	104.76 ± 1.41	7.54
	TG	TG	TG	TG	TG	TG	TG	TG
	$g(\alpha) = 0.2–0.8$	$g(\alpha) = 0.4–0.8$	$g(\alpha) = 0.2$-0.8	$g(\alpha) = 0.4–0.8$	$g(\alpha) = 0.2–0.8$	$g(\alpha) = 04–0.8$	$g(\alpha) = 0.2–0.8$	$g(\alpha) = 0.4–0.8$
II	151.09 ± 2.60	1.89×10^7	147.19 ± 5.24	2.89×10^6	149.38 ± 1.39	2.32×10^{15}	152.19 ± 6.87	6.35×10^{15}
	DSC	DSC	DSC	DSC	DSC	DSC	DSC	DSC
	$g(\alpha) = 0.2–0.8$	$g(\alpha) = 0.4–0.8$	$g(\alpha) = 0.3–0.8$	$g(\alpha) = 0.3–0.8$	$g(\alpha) = 0.2–0.8$	$g(\alpha) = 0.3–0.8$	$g(\alpha) = 0.4–0.8$	$g(\alpha) = 0.3–0.8$
III	64.42 ± 0.52	0.023	130.15 ± 14.70	579.13	64.10 ± 0.38	4.80×10^6	129.39 ± 10.43	4.21×10^{10}
	TG	TG	DSC	DSC	TG	TG	DSC	DSC
	$g(\alpha) = 0.2–0.8$	$g(\alpha) = 0.2–0.8$	$g(\alpha) = 0.4–0.8$	$g(\alpha) = 0.4–0.8$	$g(\alpha) = 0.2–0.8$	$g(\alpha) = 0.2–0.8$	$g(\alpha) = 0.4–0.8$	$g(\alpha) = 0.4–0.8$

Energetic materials	Measuring and calculation methods			
	CR			
	First thermal reaction		Second thermal reaction	
	E_a/kJ mol^{-1}	A/min^{-1}	E_a/kJ mol^{-1}	A/min^{-1}
I	106.80 ± 1.97	1.68×10^{13}	79.10 ± 0.69	4.3×10^7
	TG	TG	TG	TG
	$\beta = 5–25$ °C min^{-1}	$\beta = 5–25$ °C min^{-1}	$\beta = 5–25$ °C min^{-1}	$\beta = 5–25$ °C min^{-1}
II	377.18 ± 107.91	4.2×10^{44}	364.06 ± 13 8.30	1.88×10^{46}
	DSC	DSC	DSC	DSC
	$\beta = 0.5–2$ °C min^{-1}	$\beta = 0.5–2$ °C min^{-1}	$\beta = 0.5–2$ °C min^{-1}	$\beta = 1–2$ °C min^{-1}
III	53.82 ± 2.79	3.68×10^5	74.47 ± 8.42	4.18×10^5
	TG	TG	DSC	DSC
	$\beta = 10–25$ °C min^{-1}	$\beta = 10–25$ °C min^{-1}	$\beta = 5–25$ °C min^{-1}	$\beta = 5–25$ °C min^{-1}

Table 4 Calculated thermodynamical values of the energetic materials prepared

Energetic materials		Methods								
		KAS			OFW			CR		
		ΔH/ kJ mol^{-1}	ΔS/ J K^{-1}	ΔG/ kJ mol^{-1}	ΔH^*/ kJ mol^{-1}	ΔS/ J K^{-1}	ΔG/ kJ mol^{-1}	ΔH/ kJ mol^{-1}	ΔS/ J K^{-1}	ΔG/ kJ mol^{-1}
I	First thermal reaction	116.40	−151.05	176.52	122.07	12.68	120.48	105.04	8.20	104.01
	Second thermal reaction	94.99	−43.77	118.19	104.76	−232.93	260.21	77.14	−103.57	132.03
II	First thermal reaction	149.59	−109.08	197.08	145.59	45.74	124.77	377.18	606.00	94.82
	Second thermal reaction	143.36	−124.84	200.78	148.34	53.97	123.35	364.06	637.46	70.82
III	First thermal reaction	63.31	−269.66	174.81	62.34	−114.50	86.49	52.06	−135.50	80.65
	Second thermal reaction	125.57	−197.14	233.99	124.08	−46.61	98.44	69.89	−142.41	150.42

Table 5 Results of antimicrobial activity study

Energetic material	Bacteria					Fungus
	E. coli	*E. facealis*	*P.aeroginos*	*B. subtilis*	*S. aureus*	*C. albicans*
I						
512 mg dm^{-3}	−	−	−	−	−	−
256 mg dm^{-3}	−	−	−	−	−	−
128 mg dm^{3}	−	−	+	−	−	−
64 mg dm^{-3}	+	−	+	−	+	−
32 mg dm^{-3}	+	+	+	−	+	−
16 mg dm^{-3}	+	+	+	−	+	−
8 mg dm^{-3}	+	+	+	+	+	−
4 mg dm^{-3}	+	+	+	+	+	+
II						
512 mg dm^{-3}	+	−	+	−	−	+
256 mg dm^{-3}	+	−	+	−	−	+
128 mg dm^{3}	+	+	+	+	+	+
64 mg dm^{-3}	+	+	+	+	+	+
32 mg dm^{-3}	+	+	+	+	+	+
16 mg dm^{-3}	+	+	+	+	+	+
III						
512 mg dm^{-3}	+	−	+	−	−	−
256 mg dm^{-3}	+	−	+	−	+	−
128 mg dm^{3}	+	+	+	+	+	−
64 mg dm^{-3}	+	+	+	+	+	+
32 mg dm^{-3}	+	+	+	+	+	+
16 mg dm^{-3}	+	+	+	+	+	+

that the high antimicrobial activity of the compound I can be originated from the azide group. There are studies in the literature on antimicrobial activities of coordination compounds and heterocycle compounds containing azide groups [42–44]. It has been reported in these studies that the antimicrobial activity of the azide group is high. Is this

high activity unique to azide group or is originated from tense molecule? In order to be able to answer this question, the data in this study are not enough.

Conclusions

Nucleophilic substitution reactions and three new energetic substances have been prepared from 2,6-dinitro-4-cyanochlorobenzene, similar to picrylchloride. The free formation enthalpies of these materials were calculated from the elements using the Gaussian 09 program. Explosion products were estimated using mass spectrometry fragments, and the burst enthalpy of the energetic substance was theoretically calculated according to the Hess Law using these data. The experimental explosion was measured as enthalpy with DSC, and the values were compared. The GBS-4M algorithm in Gaussian 09 packaged software was found to be very successful in the free formation enthalpy calculation. In addition to thermal kinetic analysis, the biological activities of these substances were examined. CBS-4M calculations showed that the tension in the molecule increased antimicrobial activity.

Acknowledgements This work was supported by the Scientific Research Fund of the University of Ankara (project no. 16H0430004) and Scientific Research Fund of the Ahi Evran University (grant no: FEF.A4.17.001).

References

1. Agrawal JP, Hodgson RD. Organic chemistry of explosives. Sussex: John Wiley and Sons; 2006. p. 158–62.
2. Agrawal JP, Surve RN, Mehilal Sonawane SH. Some aromatic nitrate esters: synthesis, structural aspects, thermal and explosive properties. J Hazard Mater. 2000;77:11–31.
3. Agrawal JP. High energy materials. Weinheim: Wiley; 2010. p. 93.
4. Badgujar DM, Talawar MB, Harlapur SF, Asthana SN, Mahulikar PP. Synthesis, characterization and evaluation of 1,2-bis(2,4,6-trinitrophenyl) hydrazine. J Hazard Mater. 2009;172:276–9.
5. Yiğiter AÖ, Atakol MK, Aksu ML, Atakol O. Thermal characterization and theoretical and experimental comparison of picryl chloride derivatives of heterocyclic energetic compounds. J Therm Anal Calorim. 2017;127:2199–213.
6. Atakol M, Atakol A, Yiğiter AÖ, Svoboda I, Atakol O. Investigation of energetic materials prepared by reactions of diamines with picryl chloride: synthesis, structure and thermal behaviour. J Therm Anal Calorim. 2017;127:1931–40.
7. Klapötke TM. Chemsitry of high-energy materials. Berlin: Walter de Gruyter; 2012. p. 141–64.
8. Politzer P, Murray JS. Energetic materials part 1. Decomposition, crystal and molecular properties. Amsterdam: Elsevier; 2003. p. 411–6.
9. Badgujar DM, Talawar MB, Asthana SN, Mahulikar PP. Advances in science and technology of modern energetic materials: an overview. J Hazard Mater. 2008;151:289–305.
10. Bailey AS, Case JR. 4:6-dinitrobenzofuroxan, nitrobenzodifuroxan and benzotrifuroxan: a new series of complex-forming reagents for aromatic hydrocarbons. Tetrahedron. 1958;3:113–31.
11. Reddy GO, Murall BKM, Chotterjee AK. Thermal study on picryl azide (2-azido-1,3,5-trinitrobenzene) decomposition using simultaneous thermogravimetry and differential scanning calorimetry. Propellant Explos Pyrotech. 1983;8:29–33.
12. Shremetev AB, Aleksandrova NS, Ignat NV, Schulte M. Straightforward one-pot synthesis of benzofuroxans from o-halonitrobenzenes in ionic liquids. Mendeleev Commun. 2012;22:95–7.
13. Cardillo P, Gigante L, Lunghi A, Zanirato P. Revisiting the thermal decomposition of five ortho-substituted phenyl azides by calorimetric technics. J Therm Anal Calorim. 2010;100:191–8.
14. Fu XL, Fan XZ, Wang BZ, Huo H, Li JZ, Hu RZ. Thermal behavior, decomposition mechanism and thermal safety of 5,7-diamino-4,6-dinitrobenzofuroxan (CL-14). J Therm Anal Calorim. 2016;124:993–1001.
15. Özkaramete E, Şenocak N, İnal EK, Öz S, Svoboda I, Atakol O. Experimental and computational studies on the thermal degradation of nitroazidobenzenes. Propellant Explos Pyrotech. 2013;38:113–9.
16. Atkins P, Paula JD. Atkin's physical chemistry. 8th ed. Oxford: Oxford University Press; 2006. p. 45.
17. Coats AW, Redfern JP. Kinetic parameters from thermogravimetrical data. Nature. 1964;201:68–9.
18. Ebrahimi HP, Hadi JS, Abdulnabi ZA, Bolandnazar Z. Spectroscopic, thermal analysis and DFT computational studies of Salen type Schiff base complexes. Spectrochim Acta Part A. 2014;117:485–92.
19. Abdel-Kader NS, Amin RM, El-Ansary AL. Complexes of Schiff base of benzopyran-4-one derivative. J Therm Anal Calorim. 2016;123:1695–706.
20. Ozawa T. Kinetic analysis of derivative curves in thermal analysis. J Therm Anal Calorim. 1970;2:301–24.
21. Koga N. Ozawa's kinetic method for analysing thermoanalytical curves. J Therm Anal Calorim. 2013;113:1527–41.
22. Vyazovkin S, Burnham AK, Criado JM, Perez-Maqueda LA, Popescu C, Sbirazzuoli N. ICTAC kinetics committee recommendations for performing kinetic computations on thermal analysis data. Thermochim Acta. 2011;520:1–19.
23. Çılgı GK, Çetişli H, Donat R. Thermal kinetic analysis of uranium salts. J Therm Anal Calorim. 2014;115:2007–20.
24. Kullyakool S, Danvirutai C, Siriwong K, Noisong P. Determination of kinetic triplet of the synthesized $Ni_3(PO_4)_2{\cdot}8H_2O$ by non-isothermal and isothermal kinetic methods. J Therm Anal Calorim. 2014;115:1497–507.
25. Sarada K, Muraleedharan K. Effect of addition of silver on the thermal decomposition kinetics of copper oxalate. J Therm Anal Calorim. 2016;123:643–51.
26. Ledeti I, Fuliaş A, Vlase G, Vlase T, Bercean V, Doca N. Thermal behaviour and kinetic study of some triazoles as potential anti-inflammatory agents. J Therm Anal Calorim. 2013;114:1295–305.
27. Zianna A, Vecchio S, Gdaniee M, Czapik A, Hadzidimitriou A, Lalia-Kantouri M. Synthesis, thermal analysis and spectroscopic and structural characterizations of zinc(II) complexes with salicylaldehydes. J Therm Anal Calorim. 2013;112:455–64.
28. Gaussian 09, Revision D.01. Gaussian Inc. Wallingford CT, USA, 2009.
29. Ochterski JW, Petersson GA, Montgomery JA Jr. A complete basis set model chemistry. V. Extensions to six or more heavy atoms. J Chem Phys. 1996;104:2598–619.
30. Montgomery JA Jr, Frisch MJ, Ochterski JW, Petersson GA. A complete basis set model chemistry. VII. Use of the minimum population localization method. J Chem Phys. 2000;112:6532–42.

31. Gökçınar E, Klapötke TM, Bellamy AJ. Computational study on 2,6-diamino-3,5-dinitropyrazine and its 1-oxide and 1,4-dioxide derivatives. J Mol Struct. 2010;953:18–23.
32. Politzer P, Lane P, Concha MC. Computational determination of nitroaromatic solid phase heats of formation. Struct Chem. 2004;15:468–79.
33. Chiato ZL, Klapötke TM, Mieskes F, Stierstorfer J, Weyrauther M. (Picrylamino)-1,2,4-triazole derivatives-thermal stabl explosives. Eur J Inorg Chem. 2016;956-62.
34. Nist Chemistry WebBook, webbook. nist. gov/chemistry.
35. National Committee for Clinical Laboratory Standards. Performance standards for antimicrobial susceptibility testing. VIth informational supplement. M100S9 National Committee for Clinical Laboratory Standards, Villanova, PA. 1999.
36. Coyle MB. Manual of antimicrobial susceptibility testing, MIC testing. Washington: American Society for Microbiology; 2005. p. 53–62.
37. Hadacek F, Greger H. Testing of antifungal Natural products, methadologies, comparability of results and assay choice. Phytochem Anal. 2000;11:137–47.
38. Şen N, Özkaramete E, Yılmaz N, Öz S, Svoboda IM, Akay A, Atakol O. Thermal decomposition of dinitro-chloro-azido benzenes: a comparison of theoretical and experimental results. J Energy Mater. 2014;32:1–15.
39. Sarlauskas J, Anusevicius Z, Misiunas A. Benzofuroxan (Benzo[1,2-c]1,2,5-oxadiazole N-oxide) derivatives and potential energetic materials. Central Eur J Energy Mater. 2012;9:365–86.
40. Klapötke TM. Chemsitry of high-energy materials. Berlin: Walter de Gruyter; 2012. p. 75–6.
41. Kubota N. Propellants and explosives. 2nd ed. Weinheim: Wiley; 2007. p. 36.
42. Liu QR, Xue LW, Zhao GQ. Manganese(III) complexes derived from bis-Schiff Bases. Russ J Coord Chem. 2014;40:757–63.
43. Montazerozohari M, Jahromi SM, Masoudiasl A, McArdle P. Nanostructure zinc(II) Schiff Base complexes of a N-3-tridentate ligand as new biological active agents. Spectrochim Acta A. 2015;138:517–28.
44. Gaelle DSY, Yufanyi DM, Jagan R, Agwara MO. Synthesis, characterization and antimicrobial activity of cobalt(II) and cobalt(III) complexes derived from 1,10-phenantroline with nitrate and azide co-ligands. Cogent Chem. 2016; Article number: 1253201; doi: 10.1080/23312009.2016.1253201.